Atomic and electronic structure of the nonpolar GaN($1\bar{1}00$) surface

M. Bertelli,* P. Löptien, M. Wenderoth, A. Rizzi, and R. G. Ulbrich
IV. Physikalisches Institut, Georg-August-Universität Göttingen, D-37077 Göttingen, Germany

M. C. Righi, A. Ferretti, L. Martin-Samos, and C. M. Bertoni
CNR-INFM National Center on NanoStructures and BioSystems at Surfaces (S3) and Dipartimento di Fisica, Università di Modena e Reggio Emilia, I-41100 Modena, Italy

A. Catellani
CNR-IMEM, Parco Area Delle Scienze 37a, I-43100 Parma, Italy
(Received 16 June 2009; revised manuscript received 14 August 2009; published 25 September 2009)

We present a cross-section scanning tunneling microscopy (STM), scanning tunneling spectroscopy (STS) and *ab initio* density-functional theory simulations study of the cleaved nonpolar ($1\bar{1}00$) surface (*m*-plane) of *n*-type HVPE GaN free-standing quasisubstrates. Atomically resolved empty and filled states STM topographies show that no reconstruction occurs upon cleavage, as predicted by theory. STS measurements on clean and atomically flat cleaved surfaces (defect concentration $\sigma_d \lesssim 2\times 10^{12}$ cm^{-2}) show that the Fermi energy is not pinned and the tunneling current flows through Ga-like electronic states lying outside the fundamental band gap. On surface areas with defect concentration $\sigma_d \gtrsim 3\times 10^{13}$ cm^{-2}, the Fermi energy is pinned inside the band gap in defect-derived surface states and tunneling through filled (empty) N-like (Ga-like) states takes place.

DOI: 10.1103/PhysRevB.80.115324 PACS number(s): 68.37.Ef, 73.20.−r, 71.15.Mb

I. INTRODUCTION

Wurtzite InGaN-based alloys and heterostructures grown along nonpolar or semipolar directions are the best candidates for efficient solid-state light sources in the visible, including the green wavelength range where no other material system has achieved satisfactory quantum efficiencies. Important applications are white light emitting diodes (LEDs) for energy saving illumination and green laser diodes (LDs) for full color displays.[1] Conventional III-N heterostructure devices are grown along the polar *c* axis even though their performance are strongly affected by polarization-related electric fields parallel to the growth direction.[2] Electrons and holes are pulled to opposite sides of the quantum well (QW) interfaces by the quantum-confined Stark effect. As a consequence an undesired blueshift of the emission peak with current injection is observed[3] and the external quantum efficiency of radiative electron-hole recombination is strongly reduced.[4] These drawbacks can be avoided by growing the QW along nonpolar directions, which are free from polarization electric fields,[5] as demonstrated for green LEDs and LDs grown parallel to the [$11\bar{2}0$] (Ref. 6) and [$1\bar{1}00$] (Ref. 7) directions, respectively.

A basic knowledge of the atomic structure and energetics of the growing surface is invaluable for controlled growth of device quality heterostructures. In the past combined experimental and theoretical surface studies have provided very important insights in the molecular-beam epitaxial (MBE) growth process on the GaN (0001) and ($000\bar{1}$) polar surfaces.[8–11] For GaN(0001) MBE growth very flat surfaces and interfaces are obtained under Ga-rich conditions. It has been shown theoretically that the laterally contracted Ga-bilayer structures are energetically most favorable under Ga-rich conditions.[9] Optimized heterostructure growth has been realized by *in situ* reflection high-energy electron diffraction (RHEED) that allows to identify and to maintain the Ga-bilayer at the growing surface with a high degree of control.

A fundamental understanding of the intrinsic electronic properties of the nonpolar GaN($1\bar{1}00$) surface (*m*-plane) is still missing. Existing band structure and total-energy calculations of the GaN($1\bar{1}00$) stoichiometric surface lead to discording results. Whereas Northrup and Neugebauer[12] came to the conclusion that there should be no surface states in the band gap at the center of the Brillouin zone (BZ), Segev and Van de Walle[13] obtained an unoccupied Ga dangling bond within the fundamental band gap. This latter result would imply a Fermi-level pinning in the Ga-like empty states at the ($1\bar{1}00$) surface of *n*-type GaN. The question about the existence of intrinsic empty surface states within the fundamental band gap is still open due to the lack of experimental studies on clean GaN($1\bar{1}00$) stoichiometric surfaces. GaN($1\bar{1}00$) as-grown surfaces obtained by MBE on ZnO($1\bar{1}00$) have been studied *in situ* by scanning tunneling microscopy (STM) and scanning tunneling spectroscopy (STS) experiments.[14] The measured topographies with atomic resolution on the highly stepped surface reveal reconstructed GaN($1\bar{1}00$) terraces with approximate symmetry "4×5," which are related to nonstoichiometric surfaces stabilized under Ga-rich conditions. Cleaved GaN($1\bar{1}00$) surfaces have been investigated by means of angle-resolved ultraviolet photoemission spectroscopy (ARUPS) (Ref. 15) and cross-section STM/STS measurements.[16] The ARUPS study has shown that a N dangling-bond state exists near the valence-band maximum (VBM) and the results of the tunneling experiments have been explained with Fermi-level pinning caused by a band of extrinsic surface states originated by defects and cleavage steps.

In this work we report a comprehensive study of the cleaved nonpolar ($1\bar{1}00$) surface (*m*-plane) of *n*-type HVPE

 ©2009 The American Physical Society

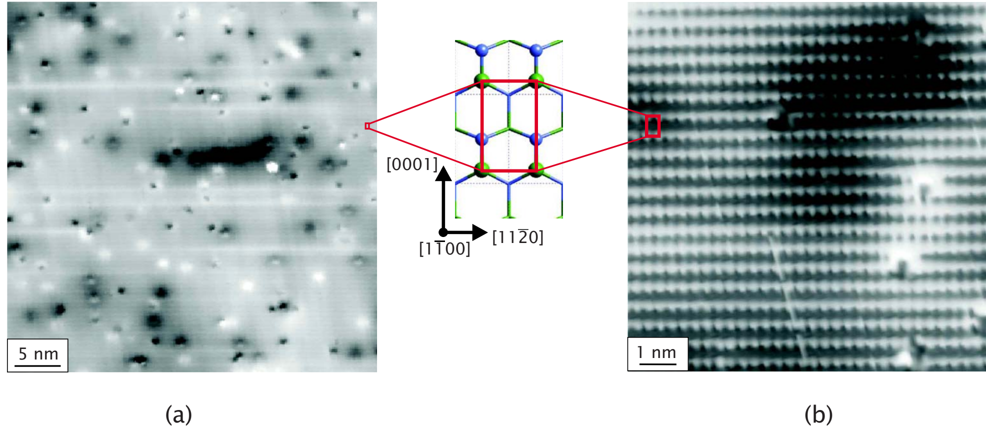

FIG. 1. (Color online) Experimental empty states STM topographies on the clean cleaved GaN(1$\bar{1}$00) surface: (a) area=40×40 nm^2, U_{bias}=+2.5 V, and I=0.05 nA; (b) area=10×10 nm^2, U_{bias}=+2.9 V, and I=0.1 nA. Gray scaled with black denoting minimal and white denoting maxima STM-tip height with the [11$\bar{2}$0] direction along x and the [0001] along y. The z range varies between (a) 0 and +110 pm and (b) 0 and +260 pm, respectively. The surface unit cell is highlighted in red (dark gray) and its stick-ball model is magnified at the center of the image: the different planes sketched are the first surface layer and the second layer in the slab. Outermost N and Ga atoms are indicated with blue (small) and green (large) spheres, respectively, while atoms in the underlayer are represented with sticks of the same colors.

free-standing GaN quasisubstrates following the same line of our previous work on the cleaved nonpolar 6H-SiC(11$\bar{2}$0) surface.[17] The atomically resolved empty and filled states STM topographies show that the cleaved GaN(1$\bar{1}$00) surface does not reconstruct, as predicted by first-principles density-functional theory (DFT) calculations. STS measurements on clean and atomically flat cleaved surfaces (defect concentration $\sigma_d \leq 2\times10^{12}$ cm^{-2}) reveal that the Fermi energy is not pinned and the tunneling current flows through Ga-like states lying outside the fundamental band gap. On cleaved surface areas with defect concentration $\sigma_d \geq 3\times10^{13}$ cm^{-2}, the Fermi energy is pinned at the surface in a band of extrinsic surface states, and the STS spectra reveal tunneling through filled N-like and empty Ga-like states.

A. Experimental details

Free-standing HVPE GaN(0001) quasisubstrates (thickness 300 μm) grown on sapphire (Al_2O_3) (LUMILOG) were cleaved in order to study the nonpolar GaN(1$\bar{1}$00) surface by STM. Direct current Hall-effect measurements were performed in van der Pauw geometry and the free-carrier concentration was determined to be $n=2.1\times10^{18}$ cm^{-3} at room temperature. The GaN samples were thinned from 300 down to about 100 μm and the N side was polished to get a mirrorlike surface. Then a scratch parallel to the [11$\bar{2}$0] direction was produced on the Ga-face of the samples in order to expose the GaN(1$\bar{1}$00) cleavage plane. Ti/Al/Ti/Au ohmic contacts were deposited on the Ga-face of the samples. Finally clean GaN(1$\bar{1}$00) surfaces were obtained by *in situ* cleavage at room temperature in UHV ($p_0 \leq 5\times10^{-11}$ mbar), and the measurements were done in a home-built Besocke-type scanning tunneling microscope.[18]

B. Theoretical details

First-principles DFT calculations were performed using the parallel version of the ESPRESSO package[19] and testing different exchange-correlation functionals from local density approximation (LDA) to Perdew-Burke-Ernzerhof[20] (PBE) approximations.[21] Wannier functions were employed to evaluate the spontaneous polarization and describe its effects at the surface.[22,23]

The single-particle wave functions were expanded in a plane-wave basis setup to a cutoff energy of 70 Ry, and all atoms were described with norm-conserving pseudopotentials; BZ sums were performed by including 16 inequivalent Monkhorst-Pack special k points in the surface BZ. We used periodically repeated symmetric supercells with up to twelve GaN layers, two atoms per layer (one Ga atom and one N atom) and a vacuum region up to 19 Å thick, to avoid interactions between replicas. We adopted this rather thick supercell to account for possible long tail reconstructions and built-in fictitious electric fields.[24] All the atoms in the slab were allowed to relax until forces were less than 10^{-4} Ryd/bohr (3 meV/Å) and the energy varied by less than 10^{-4} Ryd (1.4 meV).

II. STM/STS RESULTS

The cleavage of GaN on the (1$\bar{1}$00) plane generates surfaces characterized by terraces (mainly a few hundreds nm large) separated by steps parallel to the [0001] direction (not shown). All STM measurements were performed in constant current mode and the Fermi level of the STM tip was kept as a reference. Therefore filled and empty states STM topographies were imaged by applying to the sample negative and positive bias U_{bias}, respectively.

Figure 1 shows two empty states STM topographies on the clean and atomically flat cleaved GaN(1$\bar{1}$00) surface ($\sigma_d \approx 2\times10^{12}$ cm^{-2}): the surface unit cell shows (1×1) periodicity in agreement with the general trend of nonpolar compound semiconductor surfaces.[25] Figure 2 shows that filled and empty states in STM topographies are delocalized,

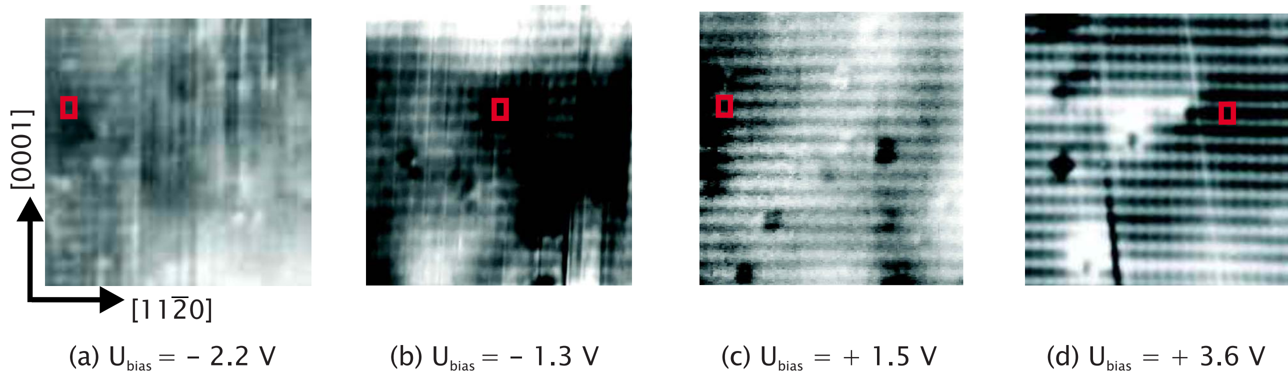

FIG. 2. (Color online) Experimental filled (a, b) and empty (c, d) states STM topographies: (a) $U_{bias}=-2.2$ V, $I=0.1$ nA, (b) $U_{bias}=-1.3$ V, $I=0.1$ nA, (c) $U_{bias}=+1.5$ V, $I=0.05$ nA, and (d) $U_{bias}=+3.6$ V, $I=0.1$ nA. Gray scaled with black denoting minimal and white denoting maxima STM-tip height (the z range is different in the images) with the $[11\bar{2}0]$ direction along x and the [0001] along y. The surface unit cell is highlighted in red (dark gray).

forming a one-dimensional chain along the $[11\bar{2}0]$ direction (from $U_{bias}=-2.2$ V to $U_{bias}=+3.6$ V).

Figure 3 shows differential conductivity dI/dU_{bias} spectra measured on the clean cleaved GaN$(1\bar{1}00)$ surface at constant bias ($U_{bias}=+1.7$ V) and different current set points I corresponding to different tip-sample distances d. The tip-sample distance decreases with increasing current set point at constant bias. The measured spectra show that a decrease in the tip-sample distance induces a contraction of the bias range where no tunneling current flows between the two electrodes. The different dI/dU_{bias} characteristics merge when the tip approaches the contact with the sample. The tunneling current vanishes ($I<1$ pA) within the bias range -1.8 V$<U_{bias}<+0.7$ V. In Sec. IV it will be shown that on the clean cleaved GaN m-plane, the tunneling current for both the filled and empty states sets on through conduction-band Ga-like states.

The results of STS measurements on the (a) clean and (b) defect-rich ($\sigma_d \approx 3\times10^{13}$ cm^{-2}) cleaved GaN$(1\bar{1}00)$ surface areas are shown in Fig. 4. The differential conductivity is represented in color scale as a function of the position along the [0001] direction (horizontal axis) and of the applied bias (vertical axis). According to the model of Hamers, the differential conductivity is proportional to the local density of states (LDOS) of the sample surface.[26] The spectra show that the maxima of empty and filled states are located at the same position on the clean cleaved GaN m-plane along the [0001] direction, while they are each other shifted of $\Delta s \approx 2$ Å on defect-rich cleaved surface areas.

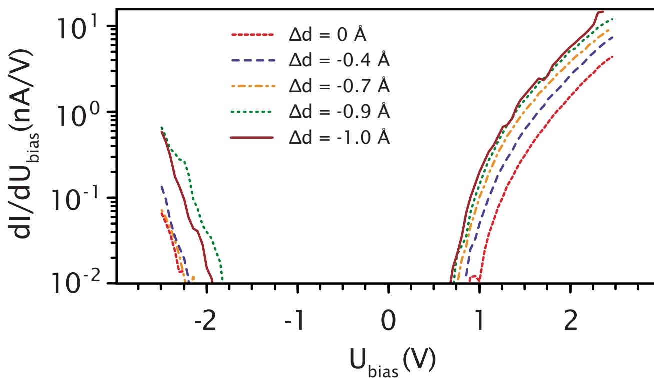

FIG. 3. (Color online) Differential conductivity dI/dU_{bias} STS spectra measured on the clean cleaved GaN$(1\bar{1}00)$ surface at constant bias $U_{bias}=+1.7$ V and different current set points I: $I=150$ pA (short-dashed red), $I=300$ pA (long-dashed blue), $I=500$ pA (dash-dotted orange), $I=700$ pA (dotted green), and $I=900$ pA (solid brown). Each spectrum is measured at different tip-sample distance $d=d_0+\Delta d$, where d_0 is the distance at set point ($U_{bias}=+1.7$ V, $I=150$ pA).

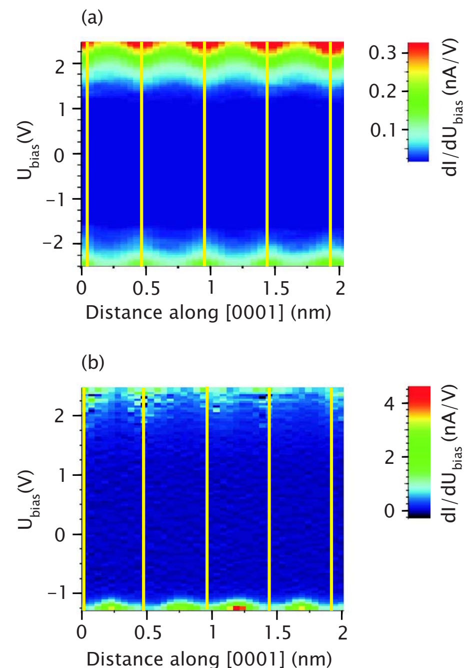

FIG. 4. (Color online) Differential conductivity STS spectra on (a) clean and (b) defect-rich cleaved GaN$(1\bar{1}00)$ surface areas taken on a line scan along the [0001] direction. Each spectrum is acquired at constant tip-sample distance according to the starting IU_{bias} set point [(a) $U_{bias}=+2.4$ V and $I=0.05$ nA, (b) $U_{bias}=+2.5$ V and $I=0.1$ nA]. The vertical yellow (light gray) lines identify the position of the empty states maxima.

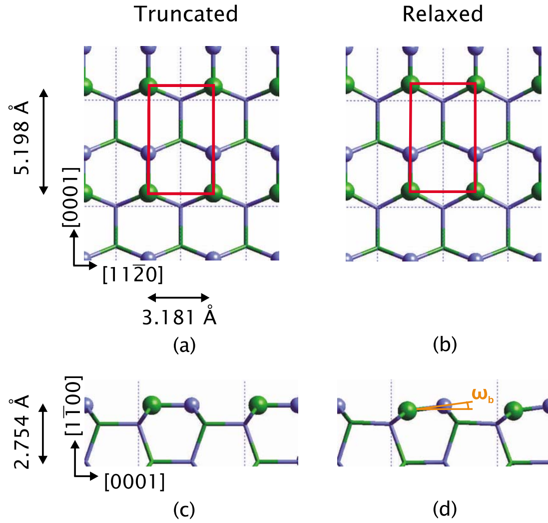

FIG. 5. (Color online) Upper images: top view of the (a) truncated and (b) relaxed supercell considered. Bottom images: side view of the (c) truncated and (d) relaxed supercell considered. The different planes sketched are the first surface layer, the second, and third layer in the slab. The buckling angle between the Ga-N surface bond and the surface plane is indicated with ω_b. Outermost N and Ga atoms are indicated with blue (small) and green (large) spheres, respectively, while atoms in the underlayer are represented with sticks of the same colors. The surface unit cell is highlighted in red (dark gray).

III. THEORETICAL ANALYSIS

As usually observed for the stoichiometric nonpolar surfaces of compound semiconductor, our *ab initio* results predict a simple relaxation mechanism for the GaN(1$\bar{1}$00) surface. In a Cartesian coordinate system the surface plane is referred to as (xy) plane, where x and y correspond to the [11$\bar{2}$0] and [0001] directions, respectively (Fig. 5). In comparison to the ideal truncated surface, the length (l) of the Ga-N bond at the surface is reduced, and a bond buckling is observed with an inward displacement (b) of the Ga atom with respect to the N atom. Within the LDA approximation we obtain a Ga-N bond length $l=1.813$ Å (corresponding to a 6.5% length reduction) and $b=0.239$ Å. The buckling angle between the Ga-N surface bond and the surface plane is $\omega_b=7.6°$. In the (xy) surface plane, an in-plane displacement is observed along the y direction: N atoms move of ≈ -0.02 Å and Ga atoms move in the opposite direction of ≈ 0.14 Å. In agreement with previous published theoretical results,[12,13,27] the LDA-DFT calculations indicate that the Ga atom moves toward an sp^2 configuration, while the N atom almost maintains its original position.

The calculated atomic structure is consistent with the electronic properties depicted in the band structure and the simulated STM images, as discussed below: upon truncation, a depletion of the Ga dangling bond with a formation of a p^* orbital and a filling of the N dangling bond occurs. The surface band structure along high-symmetry lines in the 2D BZ is shown in Fig. 6: these bands represent the eigenvalues as calculated for a 12-layer GaN slab, at the LDA lattice parameter. In the figure, the projected bulk and surface band structures are reported on the same scale: alignment has been performed taking as reference the double average of the total potential in the two calculations.[28] Apart from the $\bar{\Gamma}$ point, doubly-degenerate N-derived highest occupied (HO) and Ga-derived lowest unoccupied (LU) bands appear throughout the full BZ, as induced by the two equivalent slab surfaces. At $\bar{\Gamma}$, the bands are degenerate to the corresponding bulk band edges. Another indication that both HO and LU are resonances at $\bar{\Gamma}$, rather than true surface states, comes from inspection of the charge-density profiles of these two states (not shown). This result is consistent with the calculation of Northrup and Neugebauer,[12] but it contradicts the picture presented by Segev and Van de Walle by the use of suitably adapted pseudopotentials.[13] The various tests included beyond LDA (Ref. 21) allow us to confirm that the present picture is not dependent on the scheme that we chose for the description of d states in the calculation and on the chosen exchange-correlation functional.

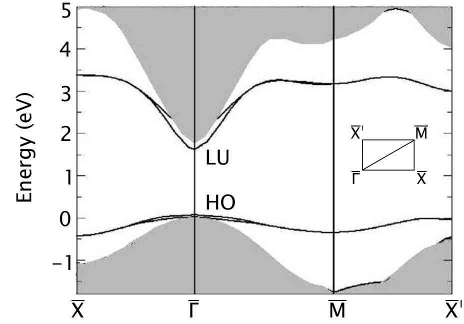

FIG. 6. Surface band structure of the relaxed GaN(1$\bar{1}$00) surface. The shaded areas show the projected bulk band structure. In the inset the projected 2D BZ is shown.

To enhance the comparison with the experimental STM measurements, we have computed STM images for filled and empty states in the Tersoff-Hamann approximation.[29] The maxima in the simulated filled [Fig. 7(a)] and empty [Fig. 7(b)] states STM topographies are localized on the N and Ga

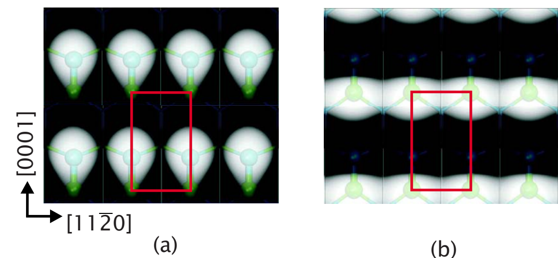

FIG. 7. (Color online) Representative simulated STM topographies for (a) filled and (b) empty states present complementary localization in space, since they are localized, respectively, on N and Ga atoms. The filled (empty) states STM topography is calculated at the $\bar{\Gamma}$ point of the BZ at $E=E_V-1.6$ eV $(E=E_C+0.3$ eV). E_V and E_C correspond to the energy of the valence-band maximum (VBM) and conduction-band minimum (CBM), respectively. Outermost N (Ga) atoms are indicated with blue (green) spheres, while atoms in the first underlayer are represented with sticks of the same colors. The surface unit cell is highlighted in red (dark gray).

atoms, respectively. The good agreement between the experimental [Fig. 1(b)] and the theoretical [Fig. 7(b)] empty states STM topographies confirms the absence of a surface reconstruction at the atomic scale.

IV. DISCUSSION

In order to specify the spatial localization of filled and empty states on the cleaved GaN *m*-plane, it is necessary to compare the theoretical predictions with the STS measurements. The DFT simulations predict for the relaxed GaN$(1\bar{1}00)$ surface the existence of a filled N-like and an empty Ga-like surface-state band resonant with the VBM and the CBM, respectively. Ivanova *et al.* suggested the absence inside the fundamental band gap of intrinsic surface states from their STS results obtained on highly defected GaN$(1\bar{1}00)$ surfaces with pinning of the Fermi level.[16] However, the only way to exclude beyond any doubt the existence of intrinsic states within the band gap is to perform STS measurements on clean cleaved GaN$(1\bar{1}00)$ surfaces on which the concentration of surface defects is not high enough to pin the Fermi energy.

Figures 1 and 2 show STM topographies on the clean and atomically flat cleaved GaN *m*-plane with a concentration of surface defects $\sigma_d \approx 2\times10^{12}$ cm^{-2}. Due to unintentional *n* doping the Fermi energy in the free-standing HVPE GaN quasisubstrates lies at $\approx$40 meV below the CBM. The differential conductivity spectra of Fig. 3 show that a decrease in the distance between STM tip and sample at constant bias set point induces a contraction of the region where no tunneling current flows between the two electrodes. By decreasing the tip-sample distance, the spectra tend to merge, defining a bias region (-1.8 V $< U_{\text{bias}} < +0.7$ V) where no electronic states are available for tunneling on the sample surface ($I < 1$ pA). A comparable dependence of the STS spectra on tip-sample distance has been observed for other nonpolar compound semiconductor surfaces on which the intrinsic surface states are located out of the fundamental band gap.[30]

The STS spectra on the clean cleaved GaN$(1\bar{1}00)$ surface at different tip-sample distances and constant bias set point have been quantitative simulated using the program IVCHAR (Ref. 31), which is based on a model of Feenstra.[30] The bending of the energy bands of the semiconductor sample is calculated in a one-dimensional model by solving consistently the Poisson equation. Then the tunneling current flowing between the sample and the STM tip through the vacuum barrier and the sample space-charge region is derived. The simulation is performed assuming a planar tip with area $A = 10$ Å^2, a value of the tip work function $\phi_T = 4.6$ eV and tunneling distances *d* from 6 to 9 Å. The simulated STS spectra reproduce quite well the experimental data with a noise floor of 1 pA (see, e.g., Fig. 9 with tip-sample distance $d = 7$ Å) and confirm that the apparent empty states band edge decreases in bias with decreasing tip-sample distance.

The experimental STS spectra of Fig. 3 show that on the clean cleaved GaN$(1\bar{1}00)$ surface the Fermi energy is not pinned and the empty Ga-like surface-state band lies outside the fundamental band gap. If an empty Ga-like surface-state band would exist inside the GaN$(1\bar{1}00)$ band gap as suggested by Segev and Van de Walle,[13] in *n*-type samples at equilibrium electrons would be transferred upon cleavage from the bulk into this empty Ga-like band. Therefore at the clean GaN$(1\bar{1}00)$ surface the Fermi level would be pinned and a significant tunneling current would arise between the STM tip and the GaN sample at small U_{bias} as in the case of the 6H-SiC$(11\bar{2}0)$ surface.[17] The STM/STS measurements support our DFT calculations and the theoretical results of Northrup and Neugebauer,[12] both predicting that the empty Ga-like surface-state band is resonant with the CBM at the $\bar{\Gamma}$ point of the BZ. Therefore we conclude that on the clean cleaved GaN$(1\bar{1}00)$ surface the empty Ga-like surface-state band is resonant with the CBM at the center of the BZ.

Figure 8 shows the tunneling model, which consistently explains the experimental STM/STS measurements on the clean and atomically flat cleaved GaN$(1\bar{1}00)$ surface and which has already been applied to other nonpolar semiconductor surfaces of *n*-type bulk material, e.g., the GaAs(110) surface, where no surface states fall inside the energy band gap at the center of the BZ.[32] In this model the tip induced band bending (TIBB) effect[30] influences the tunneling experiment. The work function of the tungsten STM tip (ϕ_T=4.5–4.8 eV) is larger than the one of the GaN sample [$\phi_S \approx \chi_S \approx 4.1$ eV, where χ_S is the value of GaN(0001) electron affinity]; therefore when the tip is brought at few Å distance from the cleaved GaN surface electrons are transferred from the GaN sample to the tip and a depletion region arises in the semiconductor close to the surface [Fig. 8(c)]. At low positive bias no tunneling current flows between sample and tip because there are no empty states in the sample which can contribute to the tunneling process [Fig. 8(d)]. Increasing the bias, the TIBB effect becomes stronger and electrons can tunnel from the Fermi energy of the tip into the empty Ga-like states of the sample [Fig. 8(e)]. At low negative bias no state is available for tunneling from the sample into the tip and the tunneling current is zero until in the sample the flat energy-band condition is reached [Fig. 8(b)]. At higher negative bias, an accumulation layer is formed at the sample surface and electrons tunnel from the filled Ga-like states of the sample into the empty states of the tip [Fig. 8(a)]. The Ga-like electronic states dominate the tunneling experiment on the clean cleaved GaN$(1\bar{1}00)$ surface and the maxima in STM topographies mark the position of Ga-like states [Figs. 1, 2, and 7(b)]. This conclusion is furthermore supported by the STS line scans of Fig. 4, which shows that the maxima of filled and empty states are located at the same position along the [0001] direction, as expected for tunneling into and out of Ga-like states by applying negative and positive bias, respectively.

The tunneling model shown in Fig. 8 for the clean cleaved GaN$(1\bar{1}00)$ surface has been quantitative simulated with the aid of the program IVCHAR, and the calculated tunneling current at tip-sample distance $d = 7$ Å as a function of the applied bias is shown in Fig. 9. The simulation shows that at positive bias the tunneling process involves empty states in the conduction band ($I_{\text{cb}}^{\text{es}}$). At negative bias it is first neces-

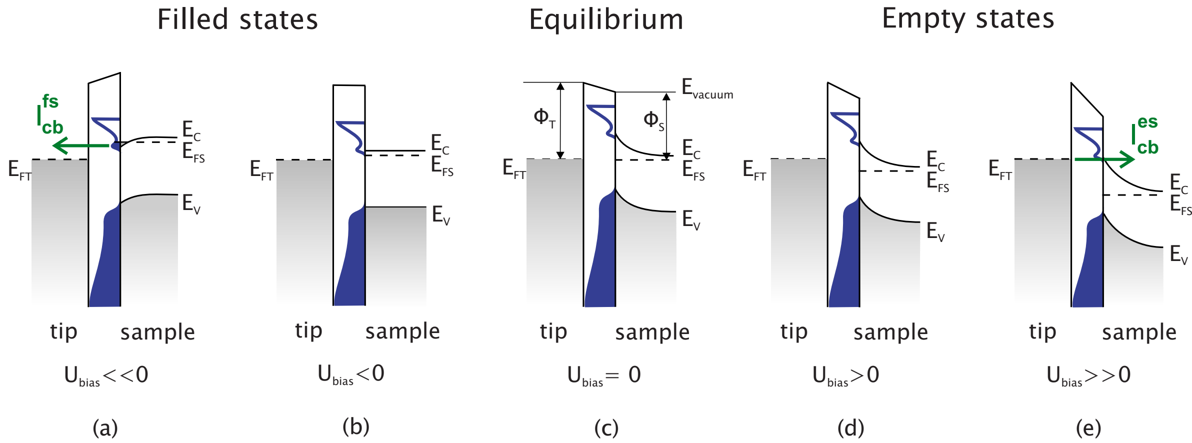

FIG. 8. (Color online) Bias-dependent scheme of the tunneling experiment on the clean cleaved GaN(1$\bar{1}$00) surface. The position of the vacuum level at equilibrium is fixed according to the work function of tungsten STM tip $\phi_T \approx 4.5-4.8$ eV and work function of n-type HVPE GaN quasisubstrates $\phi_S \approx \chi_S \approx 4.1$ eV, where χ_S represents the GaN(0001) electron affinity. The Fermi level of the tip and sample is denoted with E_{FT} and E_{FS}, respectively. E_{C} and E_{V} indicate the energy of the CBM and VBM of the sample surface, respectively. The LDOS of the sample surface is displayed in blue color (dark gray). $I_{\mathrm{cb}}^{\mathrm{fs}}$ and $I_{\mathrm{cb}}^{\mathrm{es}}$ represent the tunneling current flowing through filled and empty states of the sample conduction band, respectively.

sary to get an accumulation layer of electrons on the sample surface before the tunneling process sets on. Then at $U_{\mathrm{bias}} \approx -2.5$ V a measurable tunneling current arises involving filled states in the conduction band ($I_{\mathrm{cb}}^{\mathrm{fs}}$). Tunneling out of filled states in the valence band ($I_{\mathrm{vb}}^{\mathrm{fs}}$) sets on at $U_{\mathrm{bias}} \approx -3.8$ V, but the current is still dominated by tunneling through filled states in the conduction band. It is necessary to increase the bias up to $U_{\mathrm{bias}} = -7.5$ V so that the valence-band filled states lead the tunneling process ($I_{\mathrm{vb}}^{\mathrm{fs}} \geq I_{\mathrm{cb}}^{\mathrm{fs}}$) (not shown). The simulation shows clearly that with $-2.5\ \mathrm{V} < U_{\mathrm{bias}} < +3.5$ V tunneling through Ga-like states prevails in the experiment in agreement with the measured data and the tunneling model of Fig. 8.

N-like surface states could not be imaged in the tunneling experiment on the clean cleaved GaN m-plane. Tunneling through N-like filled states was obtained on cleaved GaN(1$\bar{1}$00) surface areas on which the concentration of surface defects was high enough to pin the Fermi level at mid-

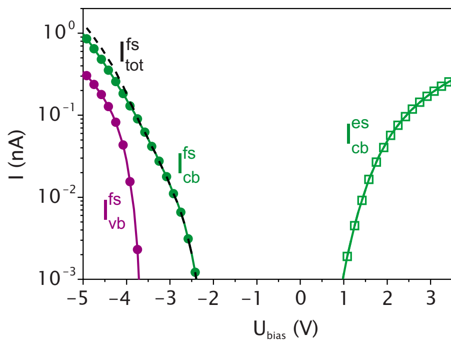

FIG. 9. (Color online) IVCHAR simulated IU_{bias} characteristic of the tunneling experiment on the clean cleaved GaN(1$\bar{1}$00) surface: $I_{\mathrm{cb}}^{\mathrm{es}}$, $I_{\mathrm{cb}}^{\mathrm{fs}}$ and $I_{\mathrm{vb}}^{\mathrm{fs}}$ are the contributions to the current due to tunneling through CB empty states, CB filled states and VB filled states, respectively. $I_{\mathrm{tot}}^{\mathrm{fs}}$ is the sum of the two contributions $I_{\mathrm{vb}}^{\mathrm{fs}}$ and $I_{\mathrm{cb}}^{\mathrm{fs}}$ to tunneling current from filled states.

gap energy. A shift $\Delta s \approx 2$ Å in the differential conductivity spectra along the [0001] direction between the maxima of filled and empty states was observed on cleaved GaN surface areas with defect density $\sigma_d \approx 3 \times 10^{13}$ cm^{-2} [Fig. 4(b)]. The tunneling model of Fig. 10 describes the experimental STM/STS results on defect-rich cleaved GaN m-plane: in n-type samples at equilibrium electrons are transferred upon cleavage from the bulk into empty defect-derived surface states and the Fermi level at the surface is pinned [Fig. 10(b)]. The observed shift $\Delta s \approx 2$ Å between empty and filled state maxima in STS spectra can be assigned to tunneling of electrons out of filled N-like surface states [Fig. 10(a)] and into empty Ga-like surface states [Fig. 10(c)].

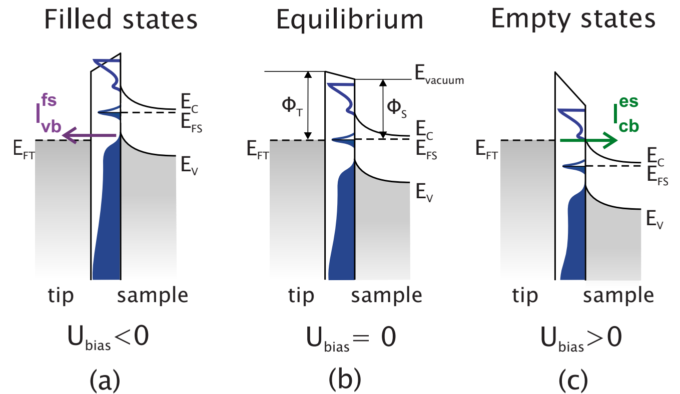

FIG. 10. (Color online) Bias-dependent scheme of the tunneling experiment on cleaved GaN(1$\bar{1}$00) surface areas with defect concentration $\sigma_d \geq 3 \times 10^{13}$ cm^{-2}. The Fermi level is pinned at the surface in defect-derived surface states. The work function of the STM-tip and sample is indicated with ϕ_T and ϕ_S, the Fermi level of the STM-tip and sample with E_{FT} and E_{FS}, respectively. E_{C} (E_{V}) denotes the energy of the CBM (VBM) of the sample. The LDOS of the sample surface is displayed in blue color (dark gray). $I_{\mathrm{vb}}^{\mathrm{fs}}$ and $I_{\mathrm{cb}}^{\mathrm{es}}$ indicate the tunneling current flowing through VB filled states and CB empty states, respectively.

V. SUMMARY AND CONCLUSIONS

The cleaved nonpolar $(1\bar{1}00)$ surface of *n*-type HVPE free-standing GaN quasisubstrates has been studied by means of cross-section STM/STS measurements and *ab initio* DFT simulations. The experimental STM topographies show an unreconstructed surface, in agreement with the theoretical calculations. The simulations show that, with respect to the ideal truncated surface, the length of the Ga-N bond at the surface is reduced and a bond buckling is observed with an inward displacement of the Ga atom with respect to the N atom.

Empty and filled states on the clean and atomically flat cleaved GaN$(1\bar{1}00)$ surface (defect concentration $\sigma_d \leq 2\times 10^{12}$ cm^{-2}) were imaged by STM with atomic resolution. The tunneling experiment can be explained in a consistent way on the basis of the TIBB effect. The STS measurements show that the Fermi energy is not pinned and the empty Ga-like surface-state band lies outside the fundamental band gap. These results are confirmed by the theory at the DFT level. In the STM/STS measurements the tunneling current for both the filled and empty states flows through conduction-band Ga-like states. The experimental data confirm the results of simulated IU_{bias} characteristics by means of a self-consistent one-dimensional Poisson solver, which show that the contribution to the tunneling current of N-like states is negligible compared to the one of Ga-like states. Tunneling through filled N-like states can be measured on cleaved GaN$(1\bar{1}00)$ surface areas where the Fermi level is pinned at midgap energy by defect-derived surface states ($\sigma_d \geq 3\times 10^{13}$ cm^{-2}).

ACKNOWLEDGMENTS

This work was partially supported by the Deutsche Forschungsgemeinschaft (Grants No. SFB 602 and No. SPP 1285), the Helmoltz Gemeinschaft—Virtual Institute of Spin Electronics (VISeL), the Ministero dell'Istruzione, dell'Università e della Ricerca (MIUR) through Grant No. PRIN 2007 BL78N3 and the INFM-CNR through the Parallel Computing Initiative. The calculations were performed using the supercomputing facilities at CINECA Bologna, Italy.

*bertelli@ph4.physik.uni-goettingen.de

[1] S. Nakamura, MRS Bull. **34**, 101 (2009).
[2] F. Bernardini, V. Fiorentini, and D. Vanderbilt, Phys. Rev. B **56**, R10024 (1997).
[3] K. S. Kim *et al.*, Appl. Phys. Lett. **92**, 101103 (2008).
[4] C. Wetzel, T. Salagaj, T. Detchprohm, P. Li, and J. S. Nelson, Appl. Phys. Lett. **85**, 866 (2004).
[5] P. Waltereit, O. Brandt, A. Trampert, H. T. Grahn, J. Menniger, M. Ramsteiner, M. Reiche, and K. H. Ploog, Nature (London) **406**, 865 (2000).
[6] T. Detchprohm, M. Zhu, Y. Li, Y. Xia, C. Wetzel, E. A. Preble, L. Liu, T. Paskova, and D. Hanser, Appl. Phys. Lett. **92**, 241109 (2008).
[7] K. Okamoto, J. Kashiwagi, T. Tanaka, and M. Kubota, Appl. Phys. Lett. **94**, 071105 (2009).
[8] T. Zywietz, J. Neugebauer, and M. Scheffler, Appl. Phys. Lett. **73**, 487 (1998).
[9] J. E. Northrup, J. Neugebauer, R. M. Feenstra, and A. R. Smith, Phys. Rev. B **61**, 9932 (2000).
[10] C. G. Van de Walle and J. Neugebauer, Nature (London) **423**, 626 (2003).
[11] C. Adelmann, J. Brault, G. Mula, B. Daudin, L. Lymperakis, and J. Neugebauer, Phys. Rev. B **67**, 165419 (2003).
[12] J. E. Northrup and J. Neugebauer, Phys. Rev. B **53**, R10477 (1996).
[13] D. Segev and C. G. Van de Walle, Europhys. Lett. **76**, 305 (2006).
[14] C. D. Lee, R. M. Feenstra, J. E. Northrup, L. Lymperakis, and J. Neugebauer, Appl. Phys. Lett. **82**, 1793 (2003).
[15] J. Wichert *et al.*, Phys. Status Solidi B **215**, 751 (1999).
[16] L. Ivanova, S. Borisova, H. Eisele, M. Dähne, A. Laubsch, and P. Ebert, Appl. Phys. Lett. **93**, 192110 (2008).
[17] M. Bertelli, J. Homoth, M. Wenderoth, A. Rizzi, R. G. Ulbrich, M. C. Righi, C. M. Bertoni, and A. Catellani, Phys. Rev. B **75**, 165312 (2007).
[18] K. Besocke, Surf. Sci. **181**, 145 (1987).
[19] P. Giannozzi *et al.*, J. Phys.: Condens. Matter **21**, 395502 (2009).
[20] J. P. Perdew, K. Burke, and M. Ernzerhof, Phys. Rev. Lett. **77**, 3865 (1996).
[21] In addition to LDA, we tested the GGA in the PBE parameterization; tests on including Hubbard and GW schemes were also considered.
[22] N. Marzari and D. Vanderbilt, Phys. Rev. B **56**, 12847 (1997) ´.
[23] A. Ferretti, B. Bonferroni, A. Calzolari, and M. Buongiorno Nardelli, WANT code, 2007 (http://www.wannier-transport.org).
[24] G. P. Brandino, G. Cicero, B. Bonferroni, A. Ferretti, A. Calzolari, C. M. Bertoni, and A. Catellani, Phys. Rev. B **76**, 085322 (2007).
[25] C. B. Duke, *Handbook of Surface Science, Physical Structure* (Elsevier, Amsterdam, 1996), Chap. 6, p. 229.
[26] R. J. Hamers, Annu. Rev. Phys. Chem. **40**, 531 (1989).
[27] A. Filippetti, V. Fiorentini, G. Cappellini, and A. Bosin, Phys. Rev. B **59**, 8026 (1999).
[28] A. J. Baldereschi, S. Baroni, and R. Resta, Phys. Rev. Lett. **61**, 734 (1988).
[29] J. Tersoff and D. R. Hamann, Phys. Rev. B **31**, 805 (1985).
[30] R. M. Feenstra and J. A. Stroscio, J. Vac. Sci. Technol. B **5**, 923 (1987).
[31] P. Koenraad, program IVCHAR, Eindhoven University of Technology.
[32] G. J. de Raad, D. M. Bruls, P. M. Koenraad, and J. H. Wolter, Phys. Rev. B **66**, 195306 (2002).